TRANSPORT OPTIMAL

Monge rencontre Riemann

ENSTA, 28 octobre 2010

Cédric Villani

Université de Lyon
& Institut Henri Poincaré

Mesure image, ou changement de variables

$\mu(dx)$, $\nu(dy)$ deux mesures (de probabilité)

$y = T(x)$

Déf: $T_{\#}\mu = \nu$ si $\forall B, \quad \mu[T^{-1}(B)] = \nu[B]$

Mesure image, ou changement de variables

$\mu(dx)$, $\nu(dy)$ deux mesures (de probabilité)

$y = T(x)$

Déf: $T_{\#}\mu = \nu$ si $\forall B, \quad \mu[T^{-1}(B)] = \nu[B]$

Équivalent: $\forall \varphi, \quad \int \varphi \circ T \, d\mu = \int \varphi \, d(T_{\#}\mu)$

Mesure image, ou changement de variables

$\mu(dx)$, $\nu(dy)$ deux mesures (de probabilité)

$y = T(x)$

Déf: $T_{\#}\mu = \nu$ si $\forall B, \quad \mu[T^{-1}(B)] = \nu[B]$

Équivalent: $\forall \varphi, \quad \int \varphi \circ T \, d\mu = \int \varphi \, d(T_{\#}\mu)$

Formulation probabiliste

$\text{loi}\,(U) = \mu, \quad \text{loi}\,(V) = \nu, \quad V = T(U)$

Mesure image, ou changement de variables

$\mu(dx)$, $\nu(dy)$ deux mesures (de probabilité)

$y = T(x)$

Déf: $T_{\#}\mu = \nu$ si $\forall B, \quad \mu[T^{-1}(B)] = \nu[B]$

Équivalent: $\forall \varphi, \quad \int \varphi \circ T \, d\mu = \int \varphi \, d(T_{\#}\mu)$

Formulation probabiliste

$\text{loi}\,(U) = \mu, \quad \text{loi}\,(V) = \nu, \quad V = T(U)$

Formulation analytique

Dans $\mathbb{R}^n$, $T_{\#}(f(x)\,dx) = g(y)\,dy$, T injective $\Rightarrow$

$f(x) = g(T(x))\,|\det(dT)(x)|$

PROBLÈME DE MONGE–KANTOROVICH

MÉMOIRE
SUR LA
THÉORIE DES DÉBLAIS ET DES REMBLAIS.

Par M. MONGE.

LORSQU'ON doit tranſporter des terres d'un lieu dans un autre, on a coutume de donner le nom de *Déblai* au volume des terres que l'on doit tranſporter, & le nom de *Remblai* à l'eſpace qu'elles doivent occuper après le tranſport.

Le prix du tranſport d'une molécule étant, toutes choſes d'ailleurs égales, proportionnel à ſon poids & à l'eſpace qu'on lui fait parcourir, & par conſéquent le prix du tranſport total devant être proportionnel à la ſomme des produits des molécules multipliées chacune par l'eſpace parcouru, il s'enſuit que le déblai & le remblai étant donnés de figure & de poſition, il n'eſt pas indifférent que telle molécule du déblai ſoit tranſportée dans tel ou tel autre endroit du remblai, mais qu'il y a une certaine diſtribution à faire des molécules du premier dans le ſecond, d'après laquelle la ſomme de ces produits ſera la moindre poſſible, & le prix du tranſport total ſera un *minimum*.

C'eſt la ſolution de cette queſtion que je me propoſe de donner ici. Je diviſerai ce Mémoire en deux parties, dans la première je ſuppoſerai que les déblais & les remblais ſont des aires contenues dans un même plan : dans le ſecond, je ſuppoſerai que ce ſont des volumes.

PREMIÈRE PARTIE.

Du tranſport des aires planes ſur des aires compriſes dans un même plan.

I.

QUELLE que ſoit la route que doive ſuivre une molécule

$\mu(dx), \nu(dy)$ deux mesures de probabilité

$c(x, y)$ fonction de coût

(MK) $\boxed{\inf_{T_{\#}\mu=\nu} \int c(x, T(x))\, d\mu(x)}$

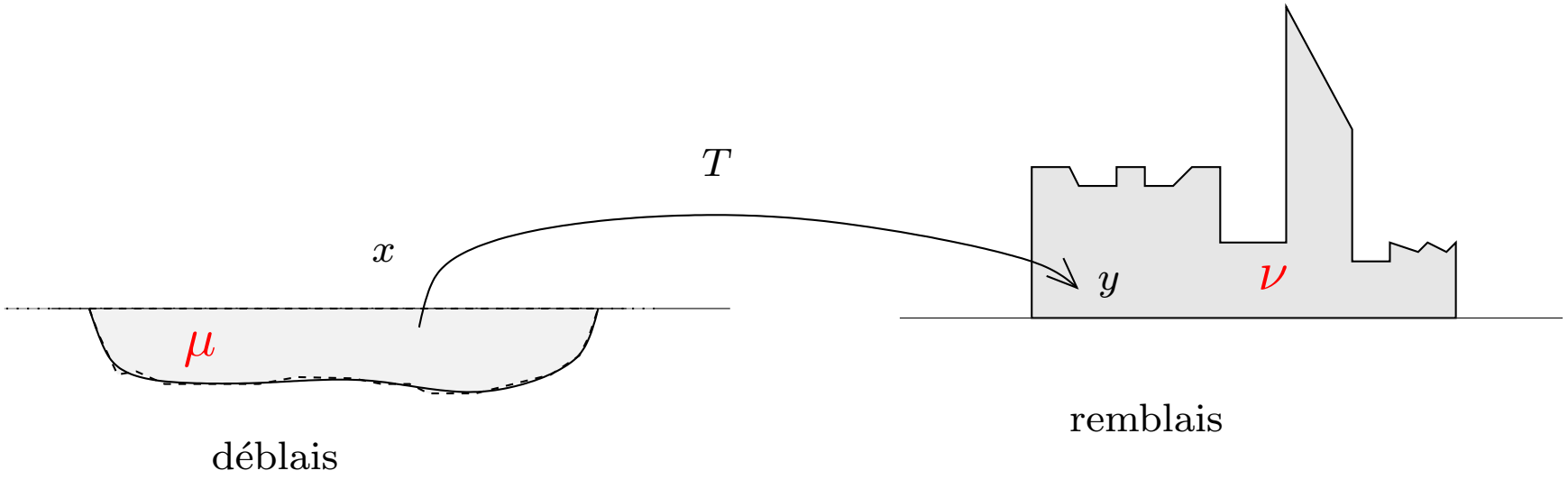

transporter des matériaux au moindre coût, distributions de masse initiale et finale fixées

Exemple: Cadre discret

$$\mu = \frac{1}{N}\sum \delta_{x_i}, \qquad \nu = \frac{1}{N}\sum \delta_{y_j}, \qquad c_{ij} = c(x_i, y_j)$$

$$\pi \simeq (\pi_{ij})_{1\leq i,j\leq N}, \qquad \sum_i \pi_{ij} = 1/N, \qquad \sum_j \pi_{ij} = 1/N$$

$\Longrightarrow N\pi$ est une matrice bistochastique

Exemple: Cadre discret

$$\mu = \frac{1}{N}\sum \delta_{x_i}, \qquad \nu = \frac{1}{N}\sum \delta_{y_j}, \qquad c_{ij} = c(x_i, y_j)$$

$$\pi \simeq (\pi_{ij})_{1\le i,j\le N}, \qquad \sum_i \pi_{ij} = 1/N, \qquad \sum_j \pi_{ij} = 1/N$$

$\Longrightarrow$ $N\pi$ est une matrice bistochastique

$$\textbf{(MK)} \qquad \boxed{\inf_{m\in\mathcal{B}_N} \sum_{ij} c_{ij}\, m_{ij}}$$

Exemple: Cadre discret

$$\mu = \frac{1}{N}\sum \delta_{x_i}, \qquad \nu = \frac{1}{N}\sum \delta_{y_j}, \qquad c_{ij} = c(x_i, y_j)$$

$$\pi \simeq (\pi_{ij})_{1\le i,j\le N}, \qquad \sum_i \pi_{ij} = 1/N, \qquad \sum_j \pi_{ij} = 1/N$$

$\Longrightarrow N\pi$ est une matrice bistochastique

$$\textbf{(MK)} \qquad \boxed{\inf_{m\in\mathcal{B}_N} \sum_{ij} c_{ij}\, m_{ij}}$$

Au moins une solution est un point extrémal de $\mathcal{B}_N$, i.e. une matrice de permutation (Théorème de Birkhoff).

$\longrightarrow$ Trouver un appariement optimal entre les x_i et les y_j

Retour au cas général

Formulation probabiliste équivalente

inf $\mathbb{E}\, c(U,V)$ parmi tous les couplages of (U,V)

Condition de Monge: $V = T(U)$

(= couplage déterministe = changement de variables)

Ex: $c(U,V) = |U-V|^2$: maximiser les corrélations
$\mathbb{E}\, U \cdot V$, chercher $V = T(U)$

Retour au cas général

Formulation probabiliste équivalente

inf $\mathbb{E}\, c(U,V)$ parmi tous les couplages of (U,V)

Condition de Monge: $V = T(U)$

(= couplage déterministe = changement de variables)

Ex: $c(U,V) = |U-V|^2$: maximiser les corrélations
$\mathbb{E}\, U \cdot V$, chercher $V = T(U)$

On peut montrer (Brenier, Rachev, Rüschendorf) que le couplage optimal prend la forme $T = \nabla\Phi$, où Φ est convexe. C'est un changement de variables monotone: la matrice jacobienne de T (= Hessienne de Φ) a ses valeurs propres positives

Les changements de variables monotones sont puissants

Isopérimétrie euclidienne

Le volume étant fixé, la sphère minimise la surface

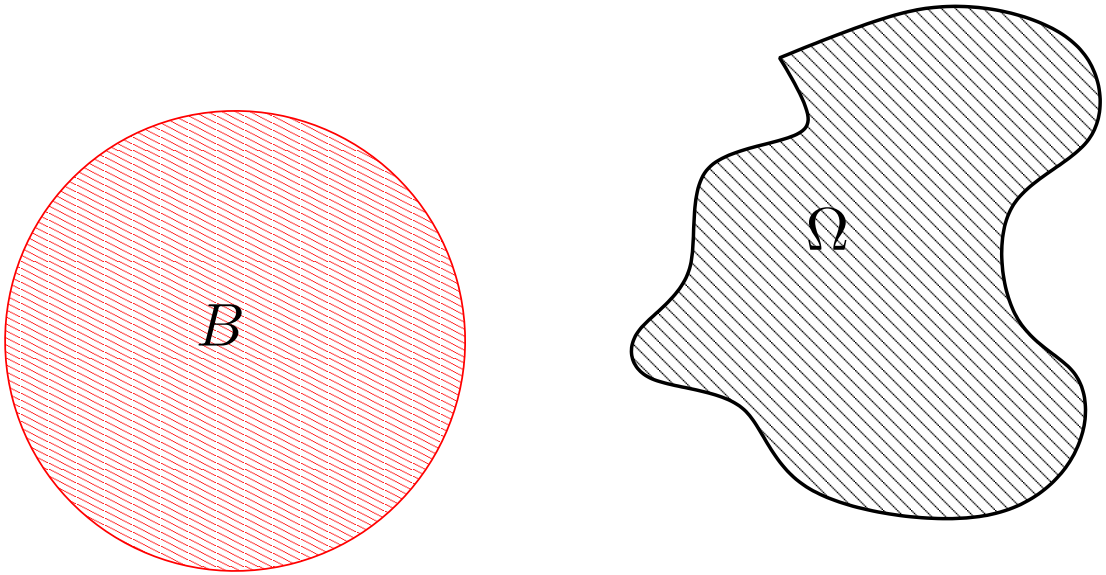

$$\begin{cases} |\Omega| = \mathcal{L}^n[\Omega] = \text{volume } n\text{-dim de } \Omega \\ \\ |\partial\Omega| = \mathcal{H}^{n-1}[\partial\Omega] = \text{volume } (n-1)\text{-dim de } \partial\Omega \end{cases}$$

$$x \in \Omega \quad \longrightarrow \quad y = T(x) \in B = B(0,1)$$

Supposons

$$\begin{cases} T \text{ transporte la mesure uniforme sur la mesure uniforme} \\ dT \textbf{ a ses valeurs propres positives} \end{cases}$$

$x \in \Omega \quad \longrightarrow \quad y = T(x) \in B = B(0,1)$

Supposons

$$\begin{cases} T \text{ transporte la mesure uniforme sur la mesure uniforme} \\ dT \textbf{ a ses valeurs propres positives} \end{cases}$$

Alors $f(x) = 1/|\Omega|$, $g(y) = 1/|B|$, donc
$\det(dT) = |B|/|\Omega|$

$x \in \Omega \quad \longrightarrow \quad y = T(x) \in B = B(0,1)$

Supposons

$$\begin{cases} T \text{ transporte la mesure uniforme sur la mesure uniforme} \\ dT \textbf{ a ses valeurs propres positives} \end{cases}$$

Alors $f(x) = 1/|\Omega|$, $g(y) = 1/|B|$, donc
$\det(dT) = |B|/|\Omega|$

$$\left(\frac{|B|}{|\Omega|}\right)^{\frac{1}{n}} = \left(\det dT\right)^{\frac{1}{n}} = \left(\prod_{i=1}^{n} \lambda_i\right)^{\frac{1}{n}} \leq \frac{\sum_{i=1}^{n} \lambda_i}{n} = \frac{\text{div } T}{n}$$

$x \in \Omega \quad \longrightarrow \quad y = T(x) \in B = B(0,1)$

Supposons

$$\begin{cases} T \text{ transporte la mesure uniforme sur la mesure uniforme} \\ dT \textbf{ a ses valeurs propres positives} \end{cases}$$

Alors $f(x) = 1/|\Omega|$, $g(y) = 1/|B|$, donc
$\det(dT) = |B|/|\Omega|$

$$\left(\frac{|B|}{|\Omega|}\right)^{\frac{1}{n}} = (\det dT)^{\frac{1}{n}} = \left(\prod_{i=1}^{n} \lambda_i\right)^{\frac{1}{n}} \leq \frac{\sum_{i=1}^{n} \lambda_i}{n} = \frac{\text{div } T}{n}$$

$$|\Omega| \times \left(\frac{|B|}{|\Omega|}\right)^{\frac{1}{n}} \leq \int_\Omega \frac{\text{div } T}{n} = \frac{1}{n} \int_{\partial\Omega} T \cdot \nu \leq \frac{1}{n} \int_{\partial\Omega} \cancel{\|T\|} = \frac{|\partial\Omega|}{n}$$

Maintenant prouvons Sobolev (Cordero–Nazaret–V 2004)

$\mathbb{R}^n, \quad 1 < p < n,$

$$\left(\int |u|^{p^\star} \right)^{1/p^\star} \leq S(n,p) \left(\int |\nabla u|^p \right)^{1/p} \qquad p^\star = \frac{np}{n-p}$$

Sans perte de généralité $u \geq 0$ et $\int u^{p^\star} = 1$: devient

$$0 < K \leq \left(\int_{\mathbb{R}^n} |\nabla u|^p \right)^{1/p}$$

$$\int g = 1, \quad T : u^{p^\star}\, dx \longrightarrow g(y)\, dy, \quad g(T(x)) = \frac{u(x)^{p^\star}}{\det(dT(x))}$$

$$\int g = 1, \quad T : u^{p^\star}\, dx \longrightarrow g(y)\, dy, \quad g(T(x)) = \frac{u(x)^{p^\star}}{\det(dT(x))}$$

$$\int g^{1-\frac{1}{n}} = \int g(y)^{-\frac{1}{n}}\, g(y)\, dy = \int g(T(x))^{-\frac{1}{n}}\, u^{p^\star}(x)\, dx$$

$$\int g = 1, \quad T : u^{p^\star} dx \longrightarrow g(y)\, dy, \quad g(T(x)) = \frac{u(x)^{p^\star}}{\det(dT(x))}$$

$$\int g^{1-\frac{1}{n}} = \int g(y)^{-\frac{1}{n}}\, g(y)\, dy = \int g(T(x))^{-\frac{1}{n}}\, u^{p^\star}(x)\, dx$$

$$= \int (\det dT(x))^{\frac{1}{n}}\, (u^{p^\star})^{1-\frac{1}{n}}\, (x)\, dx$$

$$\int g = 1, \quad T : u^{p^\star} dx \longrightarrow g(y)\, dy, \quad g(T(x)) = \frac{u(x)^{p^\star}}{\det(dT(x))}$$

$$\int g^{1-\frac{1}{n}} = \int g(y)^{-\frac{1}{n}}\, g(y)\, dy = \int g(T(x))^{-\frac{1}{n}}\, u^{p^\star}(x)\, dx$$

$$= \int (\det dT(x))^{\frac{1}{n}}\, (u^{p^\star})^{1-\frac{1}{n}}\, (x)\, dx$$

$$\leq \frac{1}{n} \int (\operatorname{div} T(x))(u^{p^\star\left(1-\frac{1}{n}\right)})(x)\, dx$$

$$\int g = 1, \quad T : u^{p^\star}\,dx \longrightarrow g(y)\,dy, \quad g(T(x)) = \frac{u(x)^{p^\star}}{\det(dT(x))}$$

$$\int g^{1-\frac{1}{n}} = \int g(y)^{-\frac{1}{n}}\, g(y)\,dy = \int g(T(x))^{-\frac{1}{n}}\, u^{p^\star}(x)\,dx$$

$$= \int (\det dT(x))^{\frac{1}{n}}\, (u^{p^\star})^{1-\frac{1}{n}}\,(x)\,dx$$

$$\leq \frac{1}{n}\int (\operatorname{div} T(x))(u^{p^\star\left(1-\frac{1}{n}\right)})(x)\,dx$$

$$= -\frac{p^\star}{n}\left(1-\frac{1}{n}\right)\int u^{p^\star\left(1-\frac{1}{n}\right)-1}\,\nabla u \cdot T\,dx$$

$$\int g = 1, \quad T : u^{p^\star}\,dx \longrightarrow g(y)\,dy, \quad g(T(x)) = \frac{u(x)^{p^\star}}{\det(dT(x))}$$

$$\int g^{1-\frac{1}{n}} = \int g(y)^{-\frac{1}{n}}\, g(y)\,dy = \int g(T(x))^{-\frac{1}{n}}\, u^{p^\star}(x)\,dx$$

$$= \int (\det dT(x))^{\frac{1}{n}}\, (u^{p^\star})^{1-\frac{1}{n}}\,(x)\,dx$$

$$\leq \frac{1}{n}\int (\operatorname{div} T(x))(u^{p^\star\left(1-\frac{1}{n}\right)})(x)\,dx$$

$$= -\frac{p^\star}{n}\left(1-\frac{1}{n}\right)\int u^{p^\star/p'} \quad \nabla u \cdot T\,dx \qquad\qquad \frac{1}{p}+\frac{1}{p'} = 1$$

$$\int g = 1, \quad T : u^{p^\star}\,dx \longrightarrow g(y)\,dy, \quad g(T(x)) = \frac{u(x)^{p^\star}}{\det(dT(x))}$$

$$\int g^{1-\frac{1}{n}} = \int g(y)^{-\frac{1}{n}}\, g(y)\,dy = \int g(T(x))^{-\frac{1}{n}}\, u^{p^\star}(x)\,dx$$

$$= \int (\det dT(x))^{\frac{1}{n}}\, (u^{p^\star})^{1-\frac{1}{n}}\,(x)\,dx$$

$$\leq \frac{1}{n}\int (\operatorname{div} T(x))(u^{p^\star\left(1-\frac{1}{n}\right)})(x)\,dx$$

$$= -\frac{p^\star}{n}\left(1-\frac{1}{n}\right)\int u^{p^\star/p'} \quad \nabla u \cdot T\,dx \qquad \frac{1}{p}+\frac{1}{p'} = 1$$

$$\leq \frac{p^\star}{n}\left(1-\frac{1}{n}\right)\left(\int u(x)^{p^\star}\,|T(x)|^{p'}\right)^{\frac{1}{p'}}\left(\int |\nabla u|^p\right)^{\frac{1}{p}}$$

$$\int g = 1, \quad T : u^{p^\star}\,dx \longrightarrow g(y)\,dy, \quad g(T(x)) = \frac{u(x)^{p^\star}}{\det(dT(x))}$$

$$\int g^{1-\frac{1}{n}} = \int g(y)^{-\frac{1}{n}}\, g(y)\,dy = \int g(T(x))^{-\frac{1}{n}}\, u^{p^\star}(x)\,dx$$

$$= \int (\det dT(x))^{\frac{1}{n}}\, (u^{p^\star})^{1-\frac{1}{n}}\,(x)\,dx$$

$$\leq \frac{1}{n}\int (\operatorname{div} T(x))(u^{p^\star\left(1-\frac{1}{n}\right)})(x)\,dx$$

$$= -\frac{p^\star}{n}\left(1-\frac{1}{n}\right)\int u^{p^\star/p'} \quad \nabla u \cdot T\,dx \qquad \frac{1}{p}+\frac{1}{p'} = 1$$

$$\leq \frac{p^\star}{n}\left(1-\frac{1}{n}\right)\left(\int u(x)^{p^\star}\,|T(x)|^{p'}\right)^{\frac{1}{p'}}\left(\int |\nabla u|^p\right)^{\frac{1}{p}}$$

$$= \frac{p^\star}{n}\left(1-\frac{1}{n}\right)\left(\int g(y)\,|y|^{p'}\right)^{\frac{1}{p'}}\left(\int |\nabla u|^p\right)^{\frac{1}{p}}$$

Développement: Inégalité isopérimétrique de Wulff isoperime

(Figalli–Maggi–Pratelli)

$\|\cdot\|$ une norme arbitraire, $\quad B = \{\|x - x_0\| \le r\}$,

$$|\partial\Omega| = \int_{\partial\Omega} \|\nu_\Omega\|_* \, \mathcal{H}^{n-1}(dx)$$

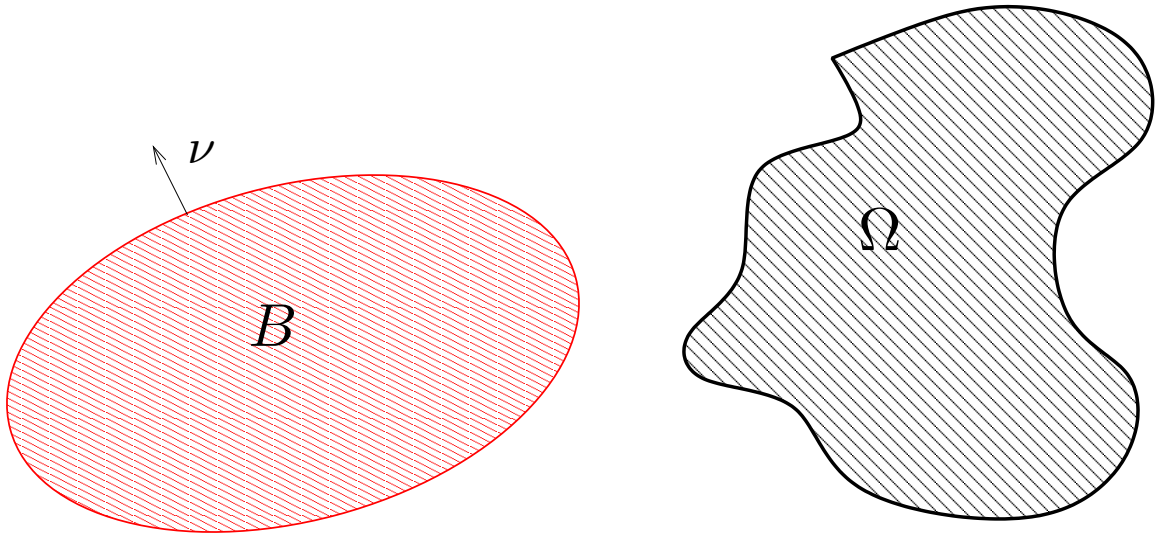

$$|\partial\Omega| \ge \inf_{|B|=|\Omega|} \left\{ |\partial B| \left(1 + \text{const.} \left(\frac{|\Omega \Delta B|}{|\Omega|} \right)^2 \right) \right\}$$

Autres applications inattendues (20 dernières années)

- mécanique des fluides incompressibles (Brenier)
- mesures invariantes syst. dynamiques (Mather)
- équations semigéostrophiques (Cullen)
- équation de Monge–Ampère (Brenier, Caffarelli)
- équation de Boltzmann (Tanaka)
- écroulement des piles de sable (Prigozhin)
- conception de réflecteurs et lentilles (Oliker, Wang)
- mise en correspondance d'images (Tannenbaum)
- modélisation de bassins d'irrigation (Santambrogio)
- reconstruction de l'univers "initial" (Frisch)
- etc.

A reconstruction of the initial conditions of the Universe by optimal mass transportation

Uriel Frisch*, Sabino Matarrese†, Roya Mohayaee‡* & Andrei Sobolevski§*

** CNRS, UMR 6529, Observatoire de la Côte d'Azur, BP 4229, 06304 Nice Cedex 4, France*
† Dipartimento di Fisica "G. Galilei" and INFN, Sezione di Padova, via Marzolo 8, 35131-Padova, Italy
‡ Dipartimento di Fisica, Universitá Degli Studi di Roma "La Sapienza", P. le A. Moro 5, 00185-Roma, Italy
§ Department of Physics, M V Lomonossov University, 119899-Moscow, Russia

Reconstructing the density fluctuations in the early Universe that evolved into the distribution of galaxies we see today is a challenge to modern cosmology[1]. An accurate reconstruction would allow us to test cosmological models by simulating the evolution starting from the reconstructed primordial state and comparing it to observations. Several reconstruction techniques have been proposed[2–9], but they all suffer from lack of uniqueness because the velocities needed to produce a unique reconstruction usually are not known. Here we show that reconstruction can be reduced to a well-determined problem of optimization, and present a specific algorithm that provides excellent agreement when tested against data from *N*-body simulations. By applying our algorithm to the redshift surveys now under way[10], we will be able to recover reliably the properties of the primeval fluctuation field of the local Universe, and to determine accurately the peculiar velocities (deviations from the Hubble expansion) and the true positions of many more galaxies than is feasible by any other method.

Starting from the available data on the galaxy distribution, can we trace back in time and map to its initial locations the highly structured distribution of mass in the Universe (Fig. 1)? Here we show that, with a suitable hypothesis, the knowledge of both the present non-uniform distribution of mass and of its primordial quasi-uniform distribution uniquely determines the inverse lagrangian map, defined as the transformation from present (eulerian) positions $\mathbf{x}$ to the respective initial (lagrangian) positions $\mathbf{q}$.

We first consider the direct lagrangian map $\mathbf{q} \mapsto \mathbf{x}$, which can be approximately written in terms of a potential as $\mathbf{x} = \nabla_{\mathbf{q}} \Phi(\mathbf{q})$ at those scales where nonlinearity stays moderate[11]. This is supported by numerical *N*-body simulations showing good agreement with a very simple potential approximation, due to Zel'dovich[12], which assumes that the particles move on straight trajectories. Even better agreement is obtained with a refinement, the second-order lagrangian perturbation method[13–16], also known to be potential.

In our 'reconstruction hypothesis', we furthermore assume the convexity of the potential $\Phi(\mathbf{q})$, a consequence of which is the absence of multi-streaming: for almost any eulerian position, there is a single lagrangian antecedent. As is well-known, the Zel'dovich approximation leads to caustics and to multi-streaming. This can be overcome in various ways, for example by a modification known as the adhesion model, an equation of viscous pressureless gas dynamics[17,18]. The latter, which leads to shocks rather than caustics, is known to have a convex potential[19] and to be in better agreement with *N*-body simulations. Suppression or reduction of multi-streaming requires a mechanism of momentum exchange, such as viscosity, between neighbouring streams having different velocities. This is a common phenomenon in ordinary fluids, such as the flow of air or water in our natural environment. Dark matter is, however, essentially collisionless, and the usual mechanism for generating viscosity (discovered by Maxwell) does not operate, so that a non-collisional mechanism involving a small-scale gravitational instability must be invoked.

Our reconstruction hypothesis implies that the initial positions can be obtained from the present ones by another gradient map: $\mathbf{q} = \nabla_{\mathbf{x}} \Theta(\mathbf{x})$, where Θ is a convex potential related to Φ by a Legendre–Fenchel transform (see Methods). We denote by ρ_0 the initial mass density (which can be treated as uniform) and by $\rho(\mathbf{x})$ the final one. Mass conservation implies $\rho_0 \, \mathrm{d}^3 q = \rho(\mathbf{x}) \, \mathrm{d}^3 x$. Thus, the ratio of final to initial density is the jacobian of the inverse lagrangian map. This can be written as the following Monge–Ampère equation[20] for the unknown potential Θ:

$$\det(\nabla_{x_i} \nabla_{x_j} \Theta(\mathbf{x})) = \rho(\mathbf{x})/\rho_0 \qquad (1)$$

where 'det' stands for determinant.

We emphasize that no information about the dynamics of matter other than the reconstruction hypothesis is needed for our method, whose degree of success depends crucially on how well this hypothesis is satisfied. Exact reconstruction is obtained, for example, for the Zel'dovich approximation (before particle trajectories cross) and for adhesion-model dynamics (at arbitrary times).

We note that our Monge–Ampère equation for self-gravitating matter may be viewed as a nonlinear generalization of a Poisson equation (used for reconstruction in ref. 4), to which it reduces if particles have moved very little from their initial positions.

It has been discovered recently that the map generated by the solution to the Monge–Ampère equation (1) is the (unique) solution to an optimization problem[21] (see also refs 22 and 23).

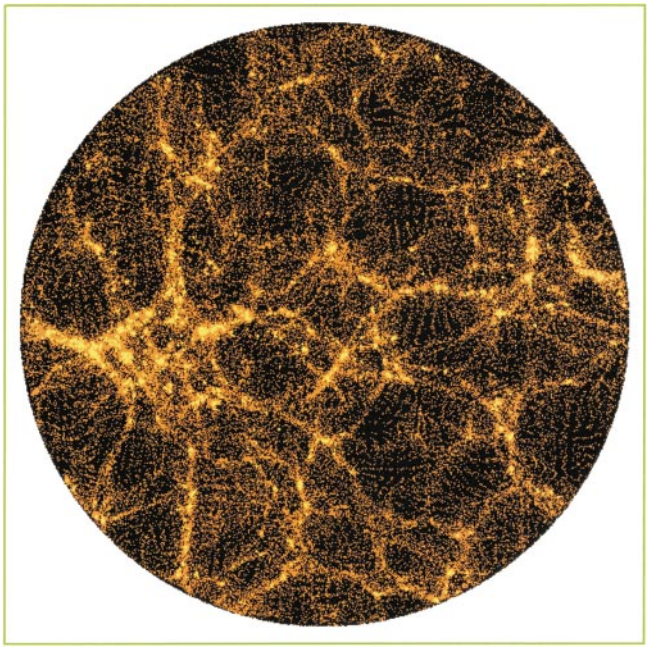

Figure 1 *N*-body simulation output (present epoch) used for testing our reconstruction method. In the standard model of structure formation, the distribution of matter in the Universe is believed to have emerged from a very smooth initial state: tiny irregularities of the gravitational potential, which we can still observe as temperature fluctuations of the cosmic microwave background, gave rise to density fluctuations, which grew under their self-gravity, developing a rich and coherent pattern of structures. Most of the mass is in the form of cold dark matter; the luminous matter (galaxies) can be assumed to trace—up to some form of bias—the underlying dark matter. Shown here is a projection onto the *x*–*y* plane of a 10% vertical slice of the simulation box of size $200\,h^{-1}$ Mpc. The model, ΛCDM, uses cold dark matter with cosmological constant and the following parameters: Hubble constant $h = 0.65$, density parameters $\Omega_\Lambda = 0.7$ and $\Omega_m = 0.3$, normalization factor $\sigma_8 = 0.99$. Points are highlighted in yellow when reconstruction fails by more than $6\,h^{-1}$ Mpc, which happens mostly in high-density regions.

This is the 'mass transportation' problem of Monge and Kantorovich[24,25], in which one seeks the map $\mathbf{x} \mapsto \mathbf{q}$ that minimizes the quadratic 'cost' function:

$$I = \int_{\mathbf{q}} \rho_0 |\mathbf{x} - \mathbf{q}|^2 \, \mathrm{d}^3 q = \int_{\mathbf{x}} \rho(\mathbf{x}) |\mathbf{x} - \mathbf{q}|^2 \, \mathrm{d}^3 x \qquad (2)$$

Note that $\mathbf{x} = \mathbf{q}$ is forbidden: as the initial and final density fields ρ_0 and $\rho(\mathbf{x})$ are prescribed, there is a constraint on the jacobian of the map (see Methods).

Next, we take into account that information on the mass distribution is provided in the form of N discrete particles both in simulations and when handling observational data from galaxy surveys. The cost minimization then becomes what is known in optimization theory as the assignment problem: find the unique one-to-one pairing of a set of N initial points $\mathbf{q}_j$ and N final points $\mathbf{x}_i$ that minimizes $I_{\mathrm{discr}} = \sum_{i=1}^{N} |\mathbf{x}_i - \mathbf{q}_{j(i)}|^2$. An immediate consequence is that, for any subset of k pairs of initial and final points ($2 \le k \le N$), the contribution of these points to the cost function should not decrease under arbitrary permutations of initial points. This property is known to be equivalent to having a lagrangian map that is the gradient of a convex function[26].

If we restrict ourselves to interchanging just pairs ($k = 2$), the map is said to be monotonic, a condition not equivalent to minimization of the cost function (except in one dimension). In ref. 5, a method of reconstruction called the path interchange Zel'dovich approximation (PIZA) is introduced, which uses the same quadratic cost function (obtained by applying a minimum-action argument within the framework of the Zel'dovich approximation). In PIZA, a randomly chosen tentative correspondence between initial and final points is successively improved by swapping pairs of initial particles whenever this decreases the cost function. Eventually, a monotonic map is obtained that usually does not minimize the cost. This explains the non-uniqueness of PIZA reconstruction (also noticed in ref. 8).

There are, however, known deterministic strategies for the assignment problem that give the correct unique solution; their complexity (dependence on N of the number of operations needed) is close to N^3 for arbitrary cost functions, but can be sharply reduced when the cost function is quadratic. Combining the organization of data taken from Hénon's mechanical analogue machine (see ref. 27, and http://www.obs-nice.fr/etc7/henon.pdf) for solving the assignment problem with the dual simplex method of Balinski[28], we have designed an algorithm that gives the optimal assignment for about 20,000 particles in a few hours of CPU time on a fast Alpha machine. For historical reasons, we call our approach Monge–Ampère–Kantorovich or MAK (see Methods). Details of the algorithms will be given elsewhere; we merely note that, when working with the catalogues of several hundred thousand galaxies that are expected within a few years, a direct application of the assignment algorithm in its present state could require unreasonable computational resources. A mixed strategy can however be used, in which the assignment problem is solved on a coarse grid while, on smaller scales, the Monge–Ampère equation (1) is solved by a relaxation technique (adapted from ref. 23).

We tested the MAK reconstruction on data obtained by a cosmological N-body simulation with 128^3 particles, using the HYDRA code[29] (Fig. 1). Reconstruction was performed on three 32^3 grids with (comoving) meshes given by $\Delta x = 6.25\ h^{-1}$ Mpc, $\Delta x/2$ and $\Delta x/4$, where h is the Hubble constant in units of $100\ \mathrm{km\ s^{-1}\ Mpc^{-1}}$. In comoving coordinates, the typical displacement of our mass elements over one Hubble time is about $10\ h^{-1}$ Mpc. We discarded those points that, at the end of the simulation (present epoch), were not within a sphere containing about 20,000 points, a number comparable to that of currently available all-sky galaxy redshift catalogues. As the simulation

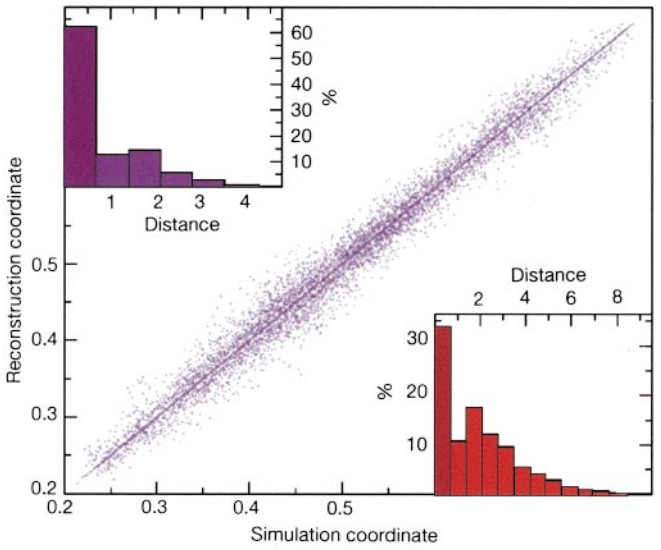

Figure 2 Tests of MAK reconstructions of the lagrangian positions, using the data shown in Fig. 1. The dots near the diagonal are a scatter plot of reconstructed initial points versus simulation initial points for the coarsest 6.25 h^{-1} Mpc grid with 17,178 points. The scatter diagram uses a 'quasi-periodic projection' coordinate $\tilde{q} \equiv (q_1 + q_2\sqrt{2} + q_3\sqrt{3})/(1 + \sqrt{2} + \sqrt{3})$, which guarantees a one-to-one correspondence between $\tilde{q}$-values and points on the regular lagrangian grid. The upper left inset is a histogram (by percentage) of distances in reconstruction mesh units between such points; the first bin (whose width was taken to be slightly less than one mesh) corresponds to perfect reconstruction (thereby allowing a good determination of the peculiar velocities of galaxies); the lower right inset is a similar histogram for reconstruction on a finer 3.12 h^{-1} Mpc grid using 19,187 points. With the 6.25 h^{-1} Mpc grid, 62% of the 17,178 points are assigned perfectly and about 75% are within not more than one mesh. With the 3.12 h^{-1} Mpc grid, we have 34% of exact reconstruction out of 19,187 points. On further refinement of the mesh by a factor of two, this degrades to 14%.

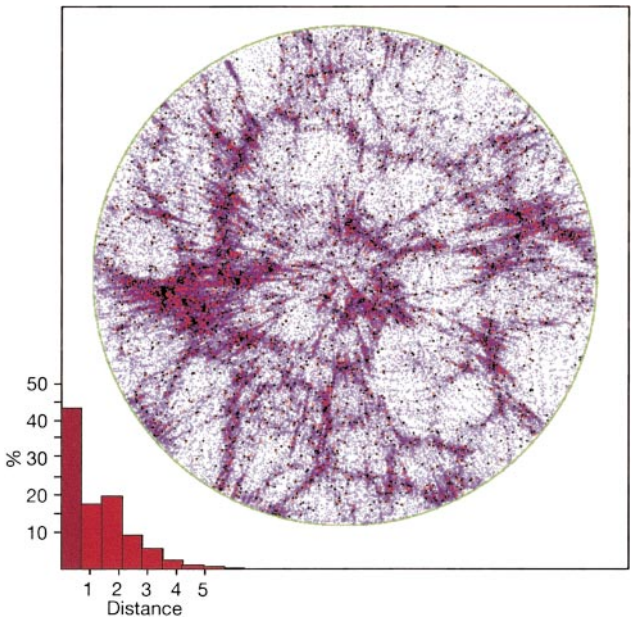

Figure 3 Reconstruction test in redshift space with the same data as for the real-space reconstruction tested in the upper left histogram of Fig. 2. The circular redshift map (violet points) corresponds to the same real-space slice as displayed in Fig. 1. The observer is taken to be at the centre of the simulation box. Points used for reconstruction within the displayed slice are highlighted in red. Reconstruction is performed by the MAK algorithm with a different cost function, obtained (as in ref. 8) by assuming that the peculiar velocities $\mathbf{v}$ can be estimated by the Zel'dovich approximation: $\mathbf{v} = f(\mathbf{x} - \mathbf{q})$, where $f \approx \Omega_{\mathrm{m}}^{0.6} \approx 0.49$. Note that we now have 43% of exactly reconstructed points, out of the 60% which are within not more than 6.25 h^{-1} Mpc from their correct positions.

assumes periodic boundary conditions, we also took into account periodicity when calculating the distance between pairs of points. The MAK reconstructions were used to generate a scatter diagram and various histograms allowing comparisons of simulation and reconstructed lagrangian points (Fig. 2). The results demonstrate the essentially potential character of the lagrangian map above $\sim 6\,h^{-1}$ Mpc (within the given cosmological model).

We also performed PIZA reconstructions on the coarsest grid, and obtained typically 30–40% exactly reconstructed points, but severe non-uniqueness: for two different seeds of the random generator, only about half of the exactly reconstructed points were the same.

When reconstructing from observational data, in redshift space (Fig. 3), the galaxies appear displaced radially (as seen by the observer) by an amount proportional to the radial component of the peculiar velocity. We thus performed another reconstruction, with an accordingly modified cost function, that led to somewhat degraded results (Fig. 3) but at the same time provided an approximate determination of peculiar velocities. More-accurate determination of peculiar velocities can be done using second-order lagrangian perturbation theory. The effect of the catalogue selection function can be handled by standard techniques; for instance, one can assign each galaxy a 'mass' inversely proportional to the catalogue selection function[8,9].

What is the smallest length scale at which an optimization algorithm such as MAK can be expected to give a unique and reliable reconstruction? The key ingredient here is the simultaneous knowledge of the initial and present mass density fields. MAK-type reconstruction (with a suitable cost based on the equation of a self-gravitating fluid) should therefore be possible down to scales comparable to the thickness of collapsed structures, below which the hydrodynamical description ceases to be meaningful.

The fact that MAK guarantees a unique solution, and that our present reconstruction hypothesis proved to be very faithful down to 6.5 h^{-1} Mpc, makes our method very promising for the analysis of galaxy redshift surveys[10]. Reconstruction of the primordial positions and velocities of matter will allow us to test the gaussian nature of the primordial perturbations and the self-consistency of cosmological hypotheses, such as the choice of the global cosmological parameters and the assumed biasing scheme. By obtaining a point-by-point reconstruction of the specific realization that describes the observed patch of our Universe, we could distinguish between universal properties and the influence of the large-scale environment on the galaxy formation process. Moreover, reconstruction would open a new window not only onto the past but also into the present Universe: it would enable us to determine the peculiar velocities of a very large number of galaxies, using their positions in redshift catalogues. □

Methods

Monge–Ampère equation

The lagrangian map $\mathbf{q} \mapsto \mathbf{x}$ is taken to be the gradient of a convex potential $\Phi(\mathbf{q})$; therefore its inverse $\mathbf{x} \mapsto \mathbf{q}$ also has a potential representation $\mathbf{q} = \nabla_{\mathbf{x}}\Theta(\mathbf{x})$, where $\Theta(\mathbf{x})$ is again a convex function; the two potentials are Legendre–Fenchel transforms of each other (see pages 61–65 in ref. 30):

$$\Theta(\mathbf{x}) = \max_{\mathbf{q}}[\mathbf{q}\cdot\mathbf{x} - \Phi(\mathbf{q})];\ \ \Phi(\mathbf{q}) = \max_{\mathbf{x}}[\mathbf{x}\cdot\mathbf{q} - \Theta(\mathbf{x})] \qquad (3)$$

The potential Θ satisfies the Monge–Ampère equation (1), written for the first time by Ampère[20] by exploiting the property of the Legendre transformation. Note that within the more restricted framework of the Zel'dovich approximation, Θ differs just by a quadratic additive term from the eulerian velocity potential[19].

Quadratic cost function

To show that the quadratic cost minimization leads to the Monge–Ampère equation, we define the displacement field $\boldsymbol{\xi}(\mathbf{x}) \equiv \mathbf{x} - \mathbf{q}(\mathbf{x})$ and perform a variation $\delta\boldsymbol{\xi}(\mathbf{x})$ to obtain, to lowest order, the variation of the cost function $\delta I = \int_{\mathbf{x}} 2\boldsymbol{\xi}(\mathbf{x})\cdot(\rho(\mathbf{x})\delta\boldsymbol{\xi})\,\mathrm{d}^3x$. The condition that the eulerian density remains unchanged, which constrains the variation, is expressed as $\nabla_{\mathbf{x}}\cdot(\rho(\mathbf{x})\delta\boldsymbol{\xi}(\mathbf{x})) = 0$. By a simple Lagrange multiplier argument, this implies that $\boldsymbol{\xi}$ must be a gradient of some function of $\mathbf{x}$; thus, $\mathbf{q} = \mathbf{x} - \boldsymbol{\xi} = \nabla_{\mathbf{x}}\Theta(\mathbf{x})$. Furthermore, should Θ be non-convex and thus lead to multi-streaming, this would prevent the lagrangian map from being optimal.

History of mass transportation

Monge[24] posed the following problem: how to optimally move material from one place to another, knowing only its initial and final spatial distributions, the cost being a prescribed function of the distance travelled by 'molecules' of material (a linear function in Monge's original work). Kantorovich[25] showed that Monge's query was an instance of the linear programming problem, and developed for it a theory that found numerous applications in economics and applied mathematics.

Received 26 September 2001; accepted 5 April 2002.

1. Narayanan, V. K. & Croft, R. A. Recovering the primordial density fluctuations: a comparison of methods. *Astrophys. J.* **515,** 471–486 (1999).
2. Peebles, P. J. E. Tracing galaxy orbits back in time. *Astrophys. J.* **344,** L53–L56 (1989).
3. Weinberg, D. H. Reconstructing primordial density fluctuations—I. Method. *Mon. Not. R. Astron. Soc.* **254,** 315–342 (1992).
4. Nusser, A. & Dekel, A. Tracing large-scale fluctuations back in time. *Astrophys. J.* **391,** 443–452 (1992).
5. Croft, R. A. & Gaztañaga, E. Reconstruction of cosmological density and velocity fields in the Lagrangian Zel'dovich approximation. *Mon. Not. R. Astron. Soc.* **285,** 793–805 (1997).
6. Nusser, A. & Branchini, E. On the least action principle in cosmology. *Mon. Not. R. Astron. Soc.* **313,** 587–595 (2000).
7. Goldberg, D. M. & Spergel, D. N. Using perturbative least action to recover cosmological initial conditions. *Astrophys. J.* **544,** 21–29 (2000).
8. Valentine, H., Saunders, W. & Taylor, A. Reconstructing the IRAS point source catalog redshift survey with a generalized PIZA. *Mon. Not. R. Astron. Soc.* **319,** L13–L17 (2000).
9. Branchini, E., Eldar, A. & Nusser, A. Peculiar velocity reconstruction with fast action method: tests on mock redshift surveys. *Mon. Not. R. Astron. Soc.* (submitted); preprint astro-ph/0110618 at ⟨http://xxx.lanl.gov⟩ (2001).
10. Frieman, J. A. & Szalay, A. S. Large-scale structure: entering the precision era. *Phys. Rep.* **333–334,** 215–232 (2000).
11. Bertschinger, E. & Dekel, A. Recovering the full velocity and density fields from large-scale redshift-distance samples. *Astrophys. J.* **336,** L5–L8 (1989).
12. Zel'dovich, Ya. B. Gravitational instability: an approximate theory for large density perturbations. *Astron. Astrophys.* **5,** 84–89 (1970).
13. Moutarde, F., Alimi, J.-M., Bouchet, F. R., Pellat, R. & Ramani, A. Precollapse scale invariance in gravitational instability. *Astrophys. J.* **382,** 377–381 (1991).
14. Buchert, T. Lagrangian theory of gravitational instability of Friedman-Lemaitre cosmologies and the Zel'dovich approximation. *Mon. Not. R. Astron. Soc.* **254,** 729–737 (1992).
15. Munshi, D., Sahni, V. & Starobinsky, A. Nonlinear approximations to gravitational instability: a comparison in the quasi-linear regime. *Astrophys. J.* **436,** 517–527 (1994).
16. Catelan, P. Lagrangian dynamics in non-flat universes and non-linear gravitational evolution. *Mon. Not. R. Astron. Soc.* **276,** 115–124 (1995).
17. Gurbatov, S. & Saichev, A. I. Probability distribution and spectra of potential hydrodynamic turbulence. *Radiophys. Quant. Electr.* **27,** 303–313 (1984).
18. Shandarin, S. F. & Zel'dovich, Ya. B. The large-scale structure of the universe: turbulence, intermittency, structures in a self-gravitating medium. *Rev. Mod. Phys.* **61,** 185–220 (1989).
19. Vergassola, M., Dubrulle, B., Frisch, U. & Noullez, A. Burgers' equation, Devil's stair-cases and the mass distribution for large-scale structures. *Astron. Astrophys.* **289,** 325–356 (1994).
20. Ampère, A.-M. Mémoire concernant l'Application de la Théorie exposée dans le XVII^{e} Cahier du Journal de l'École Polytechnique, à l'Intégration des Équations aux différentielles partielles du premier et du second ordre. *J. École. R. Polytech.* **11,** 1–188 (1820).
21. Brenier, Y. Décomposition polaire et réarrangement monotone des champs de vecteurs. *C.R. Acad. Sci.* **305,** 805–808 (1987).
22. Gangbo, W. & McCann, R. J. The geometry of optimal transportation. *Acta Math.* **177,** 113–161 (1996).
23. Benamou, J.-D. & Brenier, Y. The optimal time-continuous mass transport problem and its augmented Lagrangian numerical resolution. *Numer. Math.* **84,** 375–393 (2000) also at ⟨http://www.inria.fr/rrrt/rr-3356.html⟩.
24. Monge, G. Mémoire sur la théorie des déblais et des remblais. *Hist. Acad. R. Sci. Paris*, 666–704 (1781).
25. Kantorovich, L. On the translocation of masses. *C.R. Acad. Sci. URSS* **37,** 199–201 (1942).
26. Rockafellar, R. T. *Convex Analysis* (Princeton Univ. Press, 1970).
27. Hénon, M. A mechanical model for the transportation problem. *C.R. Acad. Sci.* **321,** 741–745 (1995).
28. Balinski, M. L. A competitive (dual) simplex method for the assignment problem. *Math. Program.* **34,** 125–141 (1986).
29. Couchman, H. M. P., Thomas, P. A. & Pearce, F. R. Hydra: an adaptive-mesh implementation of P^{3}M-SPH. *Astrophys. J.* **452,** 797–813 (1995).
30. Arnold, V. I. *Mathematical Methods of Classical Mechanics* (Springer, Berlin, 1978).

Acknowledgements

Special thanks are due to E. Branchini (observational and conceptual aspects), Y. Brenier (mathematical aspects) and M. Hénon (algorithmic aspects and the handing of spatial periodicity and of scatter plots). We also thank J. Bec, H. Frisch, B. Gladman, L. Moscardini, A. Noullez, C. Porciani, M. Rees, E. Spiegel, A. Starobinsky and P. Thomas for comments. This work was supported by the BQR program of Observatoire de la Côte d'Azur, by the TMR program of the European Union (U.F., R.M.), by MIUR (S.M.), by the French Ministry of Education, the McDonnel Foundation, the Russian RFBR and INTAS (A.S.).

Competing interests statement

The authors declare that they have no competing financial interests.

Correspondence and requests for materials should be addressed to U.F. (e-mail: uriel@obs-nice.fr).

Rappels de base de géométrie riemannienne

- espace tangent T_xM muni d'un produit scalaire $g_x =$ métrique
- $|\,u\,|_x = \sqrt{g_x(u,u)}$
- longueur d'une courbe $L(\gamma) = \displaystyle\int_0^1 |\dot\gamma(t)|_{\gamma(t)}\,dt$
- distance: $d(x,y) = \inf\Big\{L(\gamma);\ \gamma(0)=x, \quad \gamma(1)=y\Big\}$
- géodésique: γ tq $L(\gamma) = d\big(\gamma(0),\gamma(1)\big)$

Par défaut paramétrée à vitesse constante

- volume: mesure canonique généralisant Lebesgue, fonction croissante de distance

Jordan–Kinderlehrer–Otto (1998)

Sur M variété riemannienne compacte (or $M = \mathbb{R}^n$)
il y a un lien entre

- équation de la chaleur/Fourier $\dfrac{\partial \rho}{\partial t} = \Delta \rho \quad$ sur M
- fonctionnelle H de Boltzmann: $H(\rho) = \displaystyle\int \rho \log \rho$
- transport optimal $C(\mu, \nu) = \displaystyle\inf_{T_{\#}\mu = \nu} \int d\big(x, T(x)\big)^2 \, \mu(dx)$

Comment résoudre Fourier par Monge?

Schéma flot gradient non orthodoxe. Discrétise en temps.

Du temps t au temps $t + \Delta t$: Étant donné $\rho(t)$, on

cherche $\rho(t + \Delta t) =$ minimiseur de $H(\rho) + \dfrac{C(\rho(t), \rho)}{2\,\Delta t}$

L'entropie $-H = -\int \rho \log \rho$ augmente avec t (bien sûr)

Comment résoudre Fourier par Monge?

Schéma flot gradient non orthodoxe. Discrétise en temps.

Du temps t au temps $t + \Delta t$: Étant donné $\rho(t)$, on cherche $\rho(t + \Delta t) =$ minimiseur de $H(\rho) + \dfrac{C(\rho(t), \rho)}{2\,\Delta t}$

L'entropie $-H = -\int \rho \log \rho$ augmente avec t (bien sûr)

Interpolation le long du transport optimal

L'interpolation μ_t entre μ_0 et μ_1 est obtenue en arrêtant la géodésique au temps t: $T_t(x)$ est la trajectoire de $T_0(x) = x$ à $T_1(x) = T(x)$

$\mu_t = (T_t)_{\#}\mu_0$ C'est une géodésique dans l'espace des measures de probabilité, muni de la distance $\sqrt{C}(\mu, \nu)$

Quel est le comportement de H en fct de t?

Courbure sectionnelle

Soient $u, v \in T_x M$ des vecteurs unitaires orthogonaux.

$\kappa(u, v)$ mesure la divergence "extra-euclidienne" des géodésiques: $d(\gamma_u(t), \gamma_v(t)) = \sqrt{2}\, t \left(1 - \frac{\kappa}{12} t^2 + O(t^4)\right)$

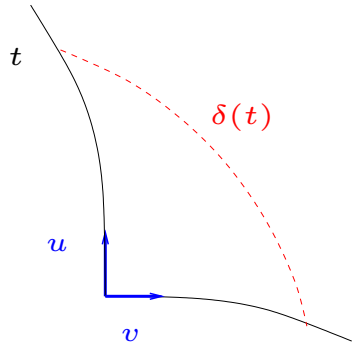

Courbure sectionnelle

Soient $u, v \in T_x M$ des vecteurs unitaires orthogonaux.
$\kappa(u,v)$ mesure la divergence "extra-euclidienne" des géodésiques: $d(\gamma_u(t), \gamma_v(t)) = \sqrt{2}\, t \left(1 - \frac{\kappa}{12}\, t^2 + O(t^4)\right)$

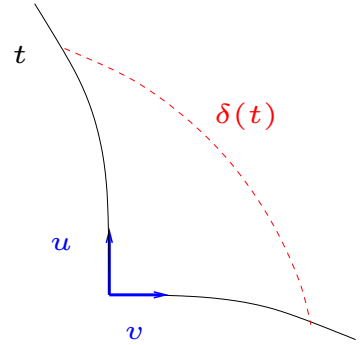

Courbure "de Ricci" = "sectionnelle moyenne"

$(e, e_2, \ldots, e_n)$ orthonormal, alors $\mathrm{Ric}(e) := \sum_{j=2}^{n} \kappa(e, e_j)$

Ceci s'étend à une forme quadratique
(exprimée en fct des dérivées secondes de la métrique g)

Relation entre transport et Ricci

$$\boxed{\mathrm{Ric} \geq 0}$$

si et seulement si

$$\boxed{H(\mu_t) = \int \rho_t \, \log \rho_t \, dx \quad \text{est une fonction convexe de } t}$$

$$\rho_t = \frac{d\mu_t}{dx}$$

(convexité le long des géodésiques du transport optimal!)

Courbure de Ricci et distortion

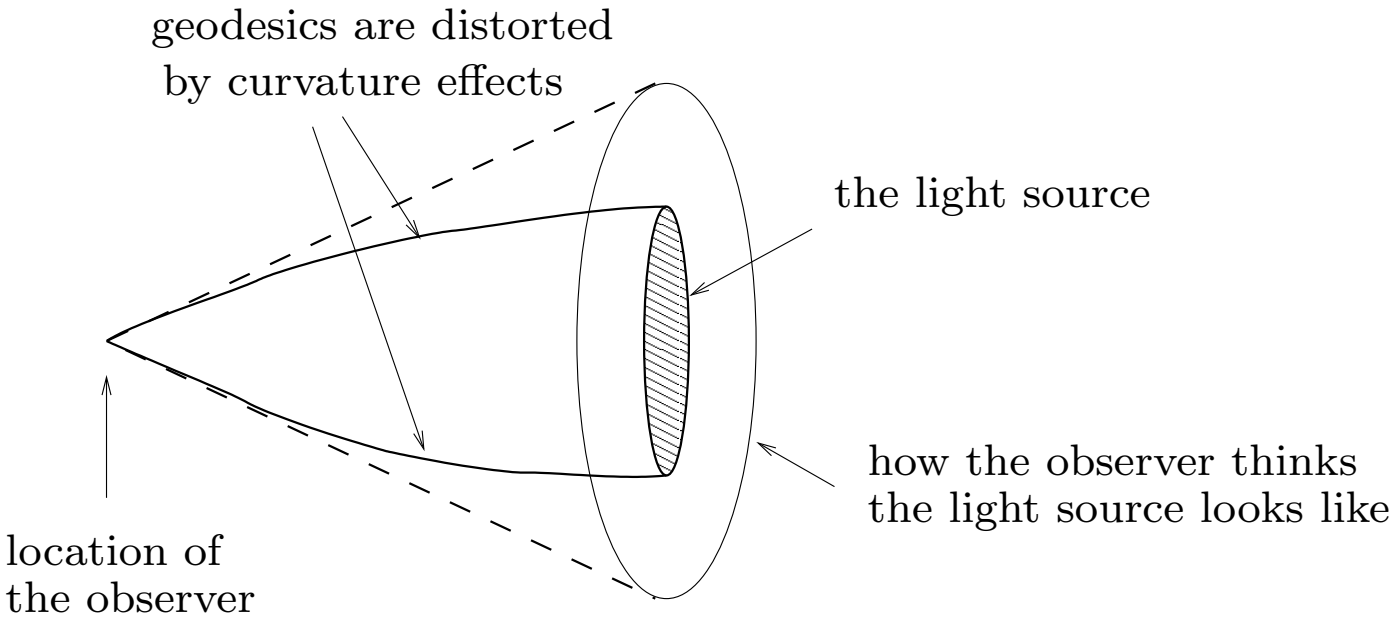

À cause de la courbure positive, l'observateur surestime la surface de la source lumineuse; en courbure négative ce serait le contraire.

$$[\text{Coefficients de distortion toujours} \geq 1] \iff [\text{Ric} \geq 0]$$

L'expérience du gaz paresseux

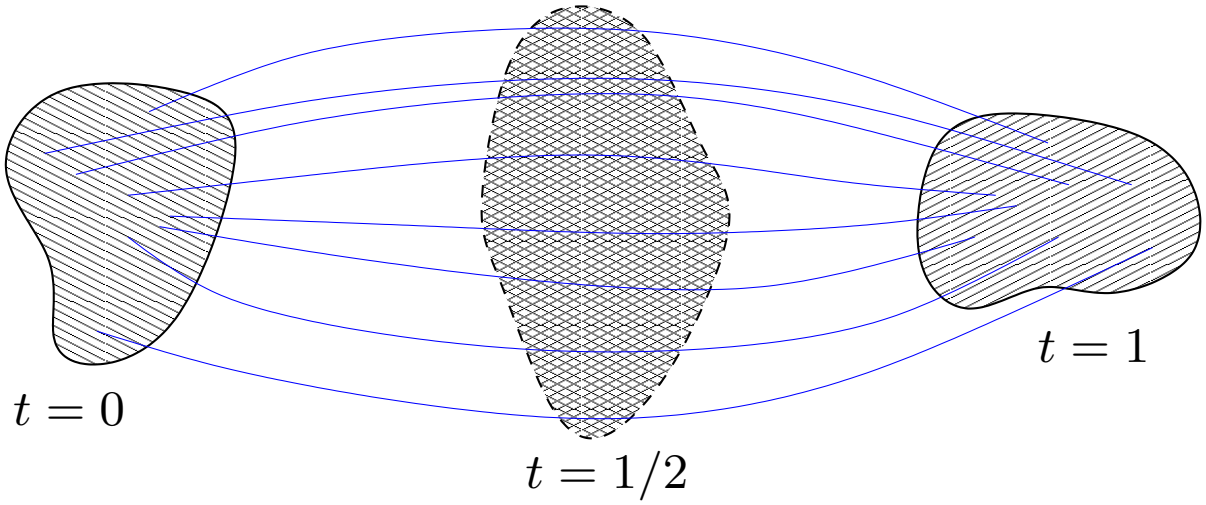

$$S = -\int \rho \log \rho$$

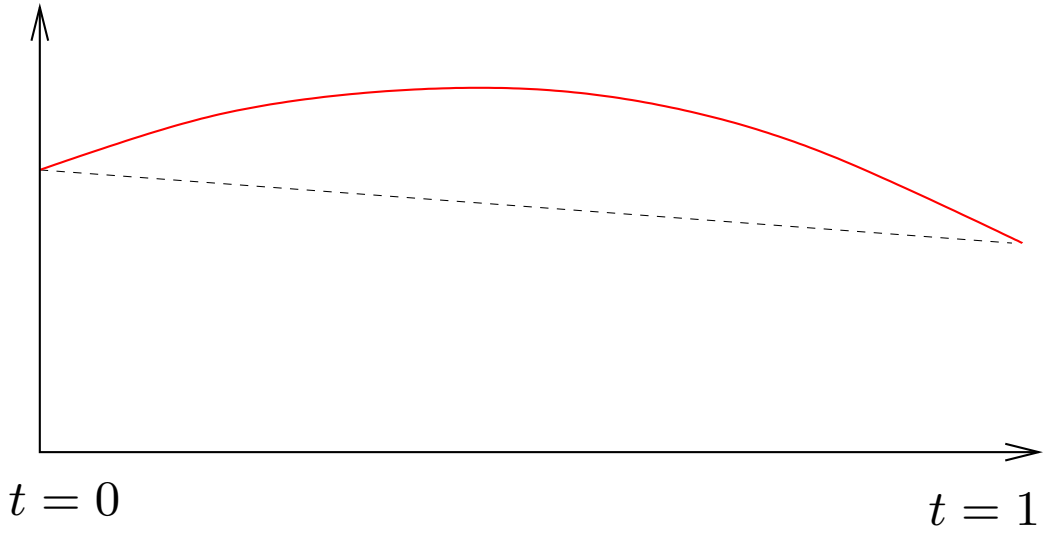

Analytique vs. Synthétique

Déf. (i) $\varphi \in C^2(\mathbb{R}^n; \mathbb{R})$ est convexe si pour tout x,

$$\nabla^2 \varphi(x) \geq 0$$

Déf. (ii) $\varphi : \mathbb{R}^n \to \mathbb{R}$ est convexe si pour tous x, y, t,

$$\varphi\big((1-t)x + ty\big) \leq (1-t)\,\varphi(x) + t\,\varphi(y)$$

(i): simple, local, effectif

(ii): utile, général, stable

Espaces métriques de courbure sectionnelle positive

(Cartan–Alexandrov–Toponogov)

$\boxed{\kappa \geq 0}$

$\Longleftrightarrow$

Triangles plus gras que triangles euclidiens

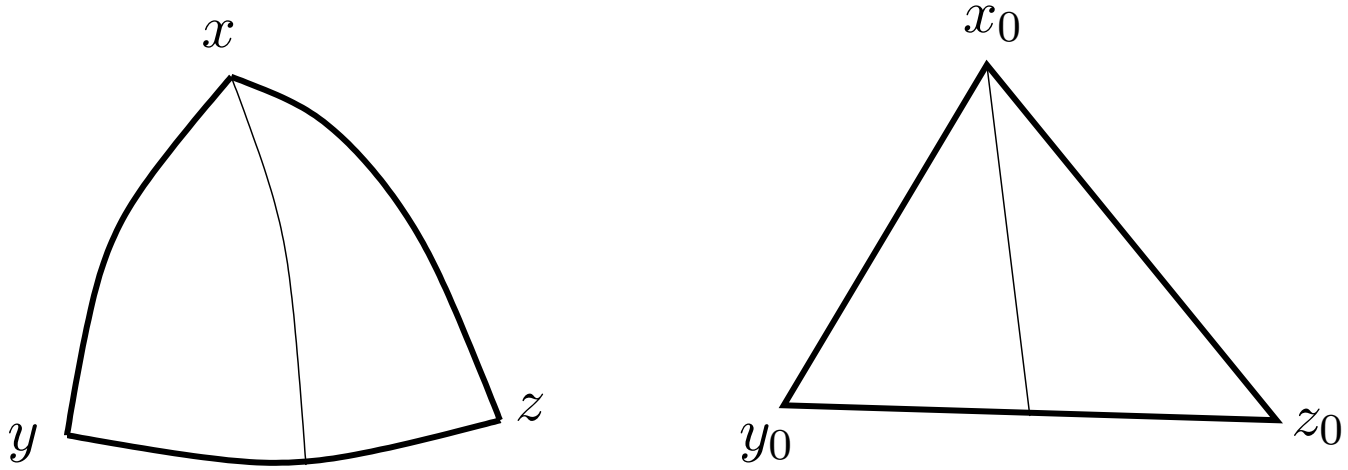

$\longrightarrow$ **espaces d'Alexandrov**

Espaces métriques de courbure sectionnelle positive

(Cartan–Alexandrov–Toponogov)

$$\boxed{\kappa \geq 0}$$

$$\Longleftrightarrow$$

Triangles plus gras que triangles euclidiens

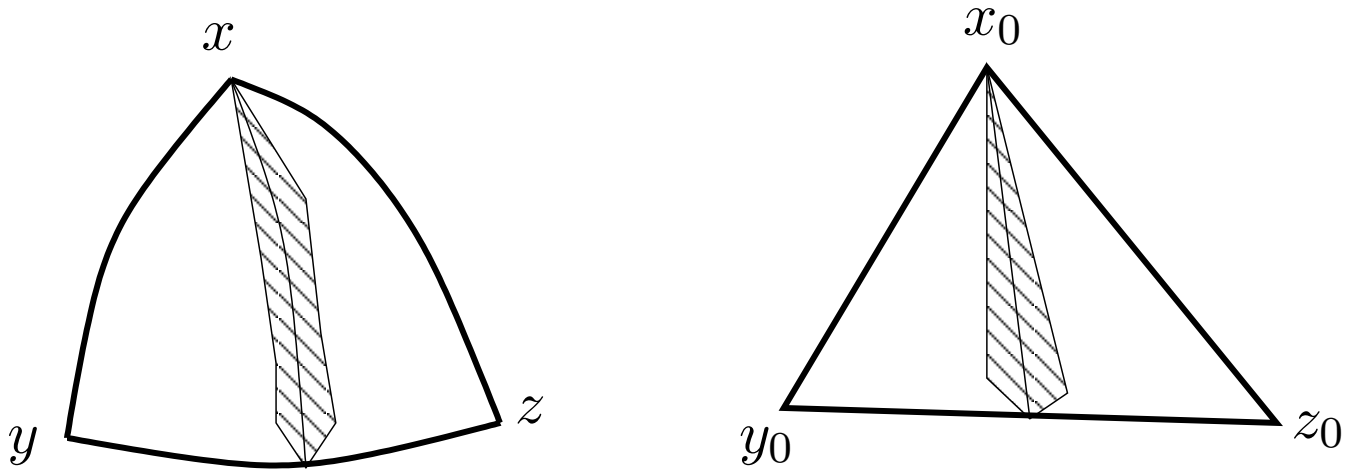

$\longrightarrow$ **espaces d'Alexandrov**

Exemple: cône

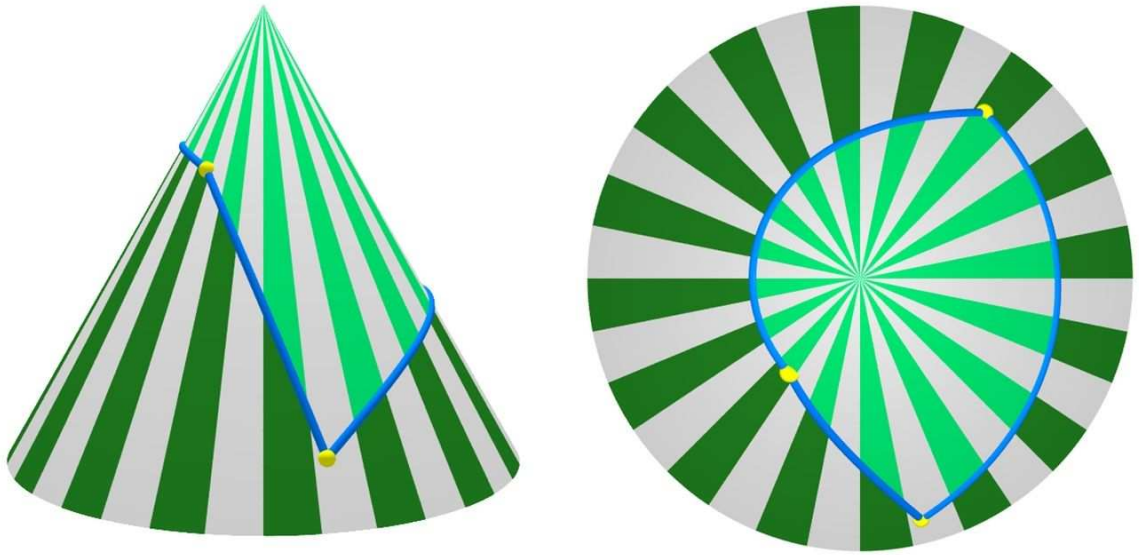

Espaces métriques à courbure de Ricci positive

(Lott–Sturm–Villani)

Déf: Un espace métrique mesuré $(\mathcal{X}, d, \nu)$ est de courbure de Ricci ≥ 0 (au sens faible/synthétique) si

$\forall \mu_0, \mu_1 \in P(\mathcal{X}) \quad \exists (\mu_t)_{0 \leq t \leq 1}, \quad$ géodésique dans $P(\mathcal{X})$, tq $\forall\, t \in [0,1]$,

$$\int \rho_t \log \rho_t \, d\nu \leq (1-t) \int \rho_0 \log \rho_0 \, d\nu + t \int \rho_1 \log \rho_1 \, d\nu$$

Espaces métriques à courbure de Ricci positive

(Lott–Sturm–Villani)

Déf: Un espace métrique mesuré $(\mathcal{X}, d, \nu)$ est de courbure de Ricci ≥ 0 (au sens faible/synthétique) si

$\forall \mu_0, \mu_1 \in P(\mathcal{X}) \quad \exists (\mu_t)_{0 \leq t \leq 1}, \quad$ géodésique dans $P(\mathcal{X})$, tq $\forall\, t \in [0,1]$,

$$\int \rho_t \log \rho_t \, d\nu \leq (1-t) \int \rho_0 \log \rho_0 \, d\nu + t \int \rho_1 \log \rho_1 \, d\nu$$

Compatibilité

La définition faible coïncide avec la définition habituelle si l'espace est lisse (variété riemannienne)

Conséquences analytiques

Par exemple Ric ≥ 0 au sens faible avec dimension N implique une inégalité de Sobolev

Stabilité

Déf: $(\mathcal{X}_k, d_k, \nu_k)_{k\in\mathbb{N}}$ converge vers $(\mathcal{X}, d, \nu)$ dans la topologie de Gromov–Hausdorff mesurée s'il y a convergence des distances et du volume. Plus précisément s'il existe $f_k : \mathcal{X}_k \to \mathcal{X}$

$$\begin{cases} \big|d(f_k(x), f_k(y)) - d_k(x,y)\big| \leq \varepsilon_k \to 0 \\ \forall x \in X, \quad d\big(x, f_k(X_k)\big) \leq \varepsilon_k \\ (f_k)_{\#}\nu_k \longrightarrow \nu \quad \text{faiblement} \end{cases}$$

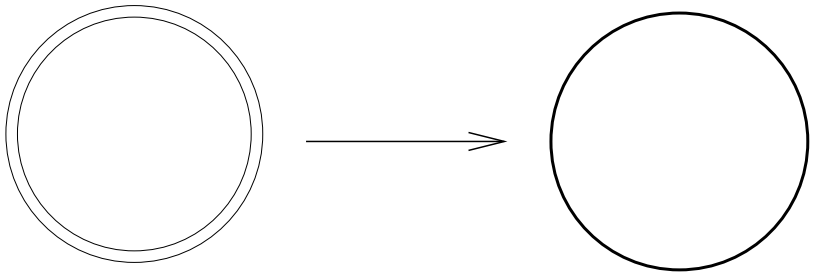

Stabilité

Déf: $(\mathcal{X}_k, d_k, \nu_k)_{k\in\mathbb{N}}$ converge vers $(\mathcal{X}, d, \nu)$ dans la topologie de Gromov–Hausdorff mesurée s'il y a convergence des distances et du volume. Plus précisément s'il existe $f_k : \mathcal{X}_k \to \mathcal{X}$

$$\begin{cases} \big|d(f_k(x), f_k(y)) - d_k(x,y)\big| \leq \varepsilon_k \to 0 \\ \forall x \in X, \quad d\big(x, f_k(X_k)\big) \leq \varepsilon_k \\ (f_k)_{\#}\nu_k \longrightarrow \nu \quad \text{faiblement} \end{cases}$$

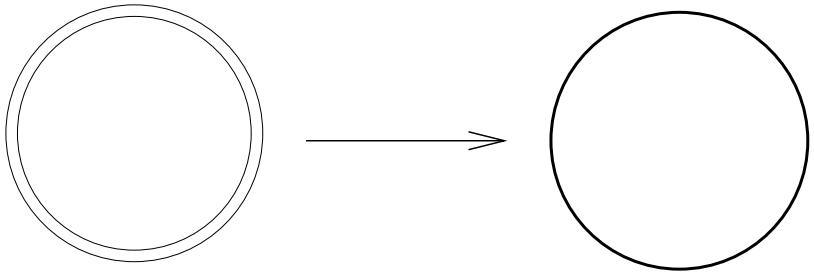

Thm: Si $(\mathcal{X}_k, d_k, \nu_k)$ sat. $\mathrm{Ric} \geq 0$ alors $(\mathcal{X}, d, \nu)$ aussi.

Compatibilité métrique (Petrunin 2009)

Si $(\mathcal{X}, d)$ est un espace d'Alexandrov compact de dimension finie avec courbure "sectionnelle" ≥ 0 alors ≥ 0 également $(\mathcal{X}, d, \mathrm{vol})$ a "Ricci" ≥ 0.

Ceci établit un lien direct entre Cartan–Alexandrov–Toponogov et Lott–Sturm–V et assure la compatibilité des définitions faibles

CONCLUSIONS

Va-et-vient entre

- mathématiques et ingénierie et physique
- analyse et probabilités et géométrie
- synthétique et analytique
- dynamique et variationnel

Les théorèmes ne se mettent pas dans des cases....

Stratégie de preuve de la stabilité

Étape 1: On reformule la condition "Ric ≥ 0":

Étant données deux mesures de probabilité μ_0 *et* μ_1 *quelconques, il y a une géodésique* $(\mu_t)_{0\leq t\leq 1}$ *dans l'espace de Wasserstein* $(P(\mathcal{X}), \sqrt{C})$, *t.q.*
$H_\nu(\mu_t) \leq (1-t)\, H_\nu(\mu_0) + t\, H_\nu(\mu_1)$

Step 2: $P_2(X)$ est stable sous MGH:

Si $f_k : X_k \to X$ *est une isométrie approchée, alors* $(f_k)_\# : P_2(X_k) \to P_2(X)$

En combinant avec un argument de compacité, on trouve une géodésique limite dans l'espace des mesures.

Step 3: Utiliser les propriétés de l'entropie pour passer à la limite dans l'inégalité

Si $U : \mathbb{R}_+ \to \mathbb{R}_+$ *est convexe continue, alors*

$$U_\nu(\mu) := \int U\left(\frac{d\mu}{d\nu}\right) d\nu$$

est semicontinue inférieurement en μ **et** ν,

et vérifie un principe de contraction:

$$\text{pour tout } f, \qquad U_{f_\#\nu}(f_\#\mu) \leq U_\nu(\mu)$$

Conclure que la même propriété est vérifiée dans l'espace limite, donc $\mathrm{Ric} \geq 0$.